Journal of Catalysis 285 (2012) 177–186

Contents lists available at SciVerse ScienceDirect

Journal of Catalysis

journal homepage: www.elsevier.com/locate/jcat

Regeneration mechanism of a Lean NO_x Trap (LNT) catalyst in the presence of NO investigated using isotope labelling techniques

Beñat Pereda-Ayo [a,b,*], Juan R. González-Velasco [a], Robbie Burch [b], Christopher Hardacre [b], Sarayute Chansai [b,*]

[a] Departamento de Ingeniería Química, Facultad de Ciencia y Tecnología, Universidad del País Vasco/Euskal Herriko Unibertsitatea, Campus de Leioa, P.O. Box 644, ES-48080 Bilbao, Bizkaia, Spain
[b] CenTACat, School of Chemistry and Chemical Engineering, Queen's University, Belfast, BT9 5AG Northern Ireland, United Kingdom

ARTICLE INFO

Article history:
Received 24 June 2011
Revised 12 September 2011
Accepted 23 September 2011
Available online 26 October 2011

Keywords:
NSR
LNT
NO_x
Reduction
Mechanism
Isotope labelling
Platinum
Barium

ABSTRACT

The presence of NO during the regeneration period of a Pt–Ba/Al_2O_3 Lean NO_x Trap (LNT) catalyst modifies significantly the evolution of products formed from the reduction of stored nitrates, particularly nitrogen and ammonia. The use of isotope labelling techniques, feeding ^{14}NO during the storage period and ^{15}NO during regeneration allows us to propose three different routes for nitrogen formation based on the different masses detected during regeneration, i.e. $^{14}N_2$ (m/e = 28), $^{14}N^{15}N$ (m/e = 29) and $^{15}N_2$ (m/e = 30). It is proposed that the formation of nitrogen via Route 1 involves the reaction between hydrogen and $^{14}NO_x$ released from the storage component to form $^{14}NH_3$ mainly. Then, ammonia further reacts with $^{14}NO_x$ located downstream to form $^{14}N_2$. In Route 2, it is postulated that the incoming ^{15}NO reacts with hydrogen to form $^{15}NH_3$ in the reactor zone where the trap has been already regenerated. This isotopically labelled ammonia travels through the catalyst bed until it reaches the regeneration front where it participates in the reduction of stored nitrates ($^{14}NO_x$) to form $^{14}N^{15}N$. The formation of $^{15}N_2$ via Route 3 is believed to occur by the reaction between incoming ^{15}NO and H_2. The modification of the hydrogen concentration fed during regeneration affects the relative importance of H_2 or $^{15}NH_3$ as reductants and thus the production of $^{14}N_2$ via Route 1 and $^{14}N^{15}N$ via Route 2.

1. Introduction

The reduction in NO_x emission from lean-burn engines has been the subject of several studies during the last decade. NO_x storage and reduction (NSR), also known as Lean NO_x Trap (LNT) catalysts, is considered to be one of the most promising technologies to solve the problem. However, most published work on LNT regeneration has been performed *in the absence of NO*. In the present work, we find that the inclusion of NO during the regeneration phase, as would occur in a real system, has a significant effect on the distribution of products.

The NSR technique was introduced by Toyota in the mid-1990s for automotive emission control [1]. A typical NSR catalyst consists of a noble metal coupled with an alkaline or alkaline-earth compound, for example Pt–BaO/Al_2O_3. The basis of this technology is to trap NO_x under lean conditions on the alkaline-earth compound (BaO) and then for the NO_x to be released and reduced to N_2 during a short rich period on the noble metal (Pt).

First studies established that the first step of the NO_x storage process is the oxidation of NO to NO_2 over platinum sites [2–6] and that NO_2 is subsequently stored on the barium component. Nova et al. [7,8] described the mechanism of NO_x storage by two routes that operate simultaneously: the "nitrite route" and the "nitrate route". The nitrite route involves the direct uptake of NO in the presence of O_2 on the barium component to form adsorbed nitrite species, which are then oxidized to nitrates. Simultaneously, the nitrate route considers the NO oxidation to NO_2, and the NO_2 formed can then adsorb on barium in the form of nitrates via a disproportionation reaction.

The regeneration step is not so well understood as the storage step. Several studies have been published on the chemistry and mechanisms that rule the reduction in NO_x ad species by H_2. The nitrate decomposition can be driven by either the heat generated from the reducing switch [9,10] or the decrease in oxygen concentration that lowers the equilibrium stability of nitrates [11,12]. However, under near isothermal conditions, it was found that the reduction process is not initiated by the thermal decomposition of the stored nitrates, but rather by a catalytic pathway involving Pt [13].

* Corresponding authors. Tel.: +34 946 012 681 (B. Pereda-Ayo), +44 289 097 4462 (S. Chansai).
E-mail addresses: benat.pereda@ehu.es (B. Pereda-Ayo), s.chansai@qub.ac.uk (S. Chansai).

0021-9517/$ - see front matter © 2011 Elsevier Inc. All rights reserved.
doi:10.1016/j.jcat.2011.09.028

More recent studies better describe both the very high selectivity to N_2 and the temporal sequence of products, with ammonia detection following that of nitrogen, in the reduction of stored NO_x by H_2 [9,14–18]. The proposed mechanism consists of a sequential two-step pathway for nitrogen formation involving the fast formation of ammonia on reaction of nitrates with H_2, followed by the slower reaction of the ammonia thus formed with the stored nitrates leading to the selective formation of N_2. For these studies, NO_x was adsorbed on the catalyst surface from a NO/O_2 stream, and then, the regeneration of the catalyst was simulated with only H_2 or NH_3 in the injected rich stream. However, in real automobile operation, NO will also be present in the gas phase during the regeneration period and this could modify the reaction network for NO_x reduction to N_2 and NH_3. The behaviour of a Pt–BaO/Al_2O_3 monolith catalyst during NO_x storage and reduction when NO is also fed together with H_2 in the regeneration period has been studied by Pereda-Ayo et al. [19,20]. This study provided information on the $N_2/N_2O/NH_3$ distribution at the exit of the trap at different temperatures and with different hydrogen concentrations. In order to obtain further insights into the complete reaction pathway governing the reduction in both stored NO_x and that fed during the regeneration period, the use of isotopically labelled NO_x has been utilized in the present study.

The use of labelled species has allowed a detailed analysis of the products and reactants involved in the regeneration of a NSR catalyst. Breen et al. [21] used isotopic labelling (^{15}NO) coupled with fast transient kinetic switching during NSR. They used ^{15}NO instead of ^{14}NO to differentiate $^{15}N_2$ from CO and $^{15}N_2O$ from CO_2 in the mass spectrometry analysis. This technique can be used to differentiate NO fed during the lean and rich periods if one of them is isotopically labelled as ^{15}NO. Kumar et al. [22] carried out isotopically labelled storage and reduction over Pt–BaO/Al_2O_3 in a TAP reactor system to elucidate the role of spillover processes and the Pt–BaO interphase during NO_x storage and reduction. The sequential pre-nitration of Pt–BaO/Al_2O_3 using NO and ^{15}NO followed by reduction with H_2 resulted in the preferential evolution of ^{15}N-containing species during the initial H_2 pulses. The evolution shifted towards unlabelled N-containing species in later H_2 pulses.

In the present study, isotopically labelled ^{15}NO is fed together with the reductant H_2 during the rich (regeneration) period while unlabelled NO is used during the lean (storage) period. The use of isotopic species helps to elucidate the different routes by which nitrogen can be formed as three different species, namely $^{14}N_2$, $^{14}N^{15}N$ and $^{15}N_2$, can be detected as products.

2. Experimental

2.1. Catalyst preparation

The γ-Al_2O_3 (SA6173) used in this study was supplied by Saint Gobain as 3-mm-diameter pellets. The as-received alumina was crushed, sieved to 0.3–0.5 mm and calcined in air at 700 °C for 4 h, resulting in a BET surface area of 190 $m^2\,g^{-1}$. The incorporation of the active phases to obtain the nominal 1.2 wt% Pt/15 wt% Ba/Al_2O_3 catalyst was carried out by adsorption from solution and wet impregnation for the platinum and barium components, respectively. The incorporation order was Pt and then Ba. First, 0.8 g of Al_2O_3 was immersed in an aqueous solution containing 650 ppm Pt with a total volume of 50 ml. The precursor used for platinum was tetraamine platinum (II) nitrate supplied by Alpha Aesar. In order to facilitate the platinum incorporation, the pH of the solution was modified by adding ammonia (25% as NH_3, Panreac) until optimum pH for platinum adsorption was obtained, i.e. a pH = 11.6 [23]. The alumina was maintained in contact with the solution for 24 h and under continuous stirring to assure that the adsorption equilibrium was obtained. Afterwards, the alumina was filtered and finally calcined in air at 500 °C for 4 h. Before incorporation of barium, the Pt/Al_2O_3 catalyst was reduced in a 5% H_2/N_2 stream at 450 °C for 2 h. The precursor used for barium incorporation was barium acetate supplied by Aldrich. After Ba incorporation via wet impregnation, the catalyst was calcined at 500 °C for 4 h.

2.2. Experimental set-up

The catalyst was evaluated using a fast transient kinetic apparatus described in more detail elsewhere [24]. Briefly, the fast switching experimental set-up was assembled using helium actuated high-speed VICI four-way valves, permitting fast feedstream changes between lean and rich cycles. The bench flow reactor consisted of a Pyrex tube enclosed in an electric furnace, and the gas mixtures used to simulate the exhaust were introduced using Aera mass flow controllers. The temperature of the catalyst bed was continuously recorded using a thermocouple located at the exit of the catalyst bed. Gas analysis was performed using a Hiden HPR 20 quadrupole mass spectrometer, the sampling inlet being positioned immediately after the catalyst bed.

2.3. NO_x storage and reduction experiments

2.3.1. Long-term NO_x storage and reduction experiments

54.9 mg of Pt–Ba/Al_2O_3 catalyst was packed in a 4-mm-internal diameter Pyrex tube. In order to follow accurately the formation of different species during catalyst regeneration, long-term NO_x storage and reduction cycles were carried out at 190 and 340 °C. The lean period was extended until the catalyst surface was saturated with NO_x, and the regeneration period was extended until complete regeneration was obtained, i.e. when N_2 and H_2O signals (main products of the regeneration) decreased to the baseline. Since the storage capacity and the regeneration pattern are dependent on the reaction temperature, the duration of lean and rich periods was 15 min and 5 min, respectively, when the temperature was set at 190 °C. When the temperature was increased to 340 °C, the duration of lean and rich periods was extended to 20 min and 7 min, respectively.

First, the influence of the presence or absence of ^{14}NO during the regeneration period was studied. When ^{14}NO was present, the regeneration feedstream consisted of 800 ppm ^{14}NO, 0.46% H_2, 5.6% Kr and balance to Ar. Kr was used as an internal standard as well as an internal marker to differentiate between lean and rich gas mixtures. In the absence of ^{14}NO during the rich period, the feedstream was composed of 0.46% H_2, 13.6% Kr and balance to Ar, maintaining the total flow rate at 130.4 ml min^{-1}, equivalent to a space velocity of 124,500 h^{-1}.

The following masses were continuously monitored to have a clear picture of the regeneration process: (m/e = 30) for ^{14}NO, (m/e = 18) for H_2O, (m/e = 28) for $^{14}N_2$, (m/e = 32) for O_2, (m/e = 46) for NO_2, (m/e = 44) for N_2O, (m/e = 2) for H_2 and (m/e = 15) for ^{14}NH, which can be attributed to the ^{14}NH fragment of $^{14}NH_3$, avoiding the overlapping of H_2O when the monitoring of ammonia is being done with the mass (m/e = 17) $^{14}NH_3$ or (m/e = 16) $^{14}NH_2$.

When ^{15}NO was admitted during regeneration instead of ^{14}NO, the composition of the feedstream was not altered: 800 ppm of ^{15}NO, 0.46% H_2, 5.6% Kr and balance to Ar. In this case, apart from the masses already reported, the following masses were also continuously monitored: (m/e = 29) for $^{14}N^{15}N$, (m/e = 30) for $^{15}N_2$ or ^{14}NO and (m/e = 31) for ^{15}NO.

2.3.2. Moving to shorter regeneration periods by increasing H_2 concentration

In order to more closely reflect real conditions, the NO_x storage and reduction experiments were carried out limiting the length of the storage and reduction periods to 2 min. During the regeneration, the higher H_2 concentration allowed us to shorten the regeneration time of the catalysts to a few seconds. The hydrogen concentration was varied from 0.46% to 3.83%, and the experiments were run with either ^{14}NO or ^{15}NO present during the regeneration.

3. Results and discussion

3.1. Effect of the presence of NO during LNT regeneration

As indicated in Introduction, most work dealing with mechanistic aspects of NO_x storage and reduction has omitted to include NO during the regeneration part of the experiments. It is important to investigate whether or not the inclusion of NO during regeneration changes the product profiles. For these experiments, the lean gas mixture composed of 800 ppm NO, 6% O_2 and Ar to balance was fed to the Pt–Ba/Al_2O_3 catalyst until saturation of NO_x. As the previous studies reported [11], the NO_x storage capacity shows a volcano-type dependence on the temperature, with a maximum typically occurring at 350 °C. Therefore, 15 min was needed to saturate the catalyst when the reaction was carried out at 190 °C, whereas 20 min was needed at 340 °C. After saturation, the feedstream was switched to rich conditions, and the catalyst regeneration was carried out in the presence or absence of 800 ppm NO along with 0.46% H_2 and Ar to balance.

During the regeneration, the evolution of different mass signals which can be assigned to different products was recorded and these are plotted in Fig. 1. Fig. 1a shows the evolution of NO ($m/e = 30$), N_2 ($m/e = 28$), NH_3 and OH ($m/e = 17$) and NH ($m/e = 15$) signals in the presence (red[1] points) and in the absence (black points) of NO when the regeneration was carried out at 190 °C. Similarly, Fig. 1b shows the evolution of N_2O ($m/e = 44$), H_2O ($m/e = 18$), H_2 ($m/e = 2$) and the exit temperature profile. The *Y* axis depicted in Figs. 1 and 2 is shown in arbitrary units except in case of temperature. The same procedure was used to investigate the NO_x reduction performance when the reaction was carried out at 340 °C (Fig. 2a and b).

As can be observed in Fig. 1a, when the rich feed is admitted to the catalyst ($t = 0$), the NO signal drops from the saturation level (300 a.u.) to below 20 a.u. in the presence and in the absence of NO. However, in the presence of NO during regeneration, a sudden release (known as "NO_x puff") is recorded at the beginning of the rich period, which is not observed in the absence of NO. Therefore, it can be concluded that when NO is admitted during regeneration, the supply of reductant is not sufficient to reduce the NO being released from the catalyst surface as well as that present in the gas stream. Simultaneously, the reduction in stored nitrates with the incoming H_2 led to the formation of N_2, NH_3, N_2O and H_2O. As can be observed in Fig. 1a and b, the formation of N_2 and N_2O is detected immediately after the rich period starts, whereas the detection of H_2O and NH_3 is delayed to some extent. The ($m/e = 18$) signal corresponding to H_2O is detected after 20 s of regeneration. At the same time, together with H_2O breakthrough, the ($m/e = 17$) signal breakthrough is detected due to the OH ($m/e = 17$) fragmentation coming from H_2O. However, if the monitoring of ammonia is carried out using the NH fragment ($m/e = 15$), it is possible to remove any contributions from mass fragmentation from other species and consequently it can be observed that NH_3 is only detected after 40 s into the regeneration.

The presence of NO during regeneration increases the total amounts of N_2, NH_3 and H_2O significantly, whereas the formation of N_2O remains practically unchanged, suggesting that stored nitrates are the only source for N_2O formation and that incoming NO does not participate in its formation. As expected, the addition of NO during the rich period increases the time needed to obtain the complete regeneration of the trap. This can be understood because apart from stored nitrates, hydrogen also has to reduce the incoming gas phase NO. Consequently, the hydrogen breakthrough is delayed for 40 s as can be observed in Fig. 1b. The complete consumption of H_2 during the initial period of the regeneration together with the rectangular shape of the H_2O formation curve indicates a "plug flow" type of mechanism. As several authors have already reported [9,14,15,25], the hydrogen front travels through the catalyst bed with complete regeneration of the trapping sites as it propagates down the bed. Those reactions, leading to the final regeneration of the trap, are exothermic, increasing the temperature of the catalyst bed from 189 °C to a maximum of 196 °C, which is coincident in time with the hydrogen breakthrough, or the end of the regeneration. After complete regeneration has been obtained, the catalyst temperature slowly decreases until the initial temperature is recovered.

In the absence of NO during regeneration, the signal corresponding to N_2, NH_3, N_2O and H_2O decreased slowly back to the baseline once the regeneration of the trap was finished. However, in the presence of NO, the signals corresponding to N_2, NH_3 and H_2O remained constant at values higher than the baseline. Thus, it can be deduced that after catalyst regeneration, when no nitrates are present in the catalyst surface, the reaction between NO and H_2 led to the formation of those products, with the production of NH_3 being more favourable than N_2 due to the low NO/H_2 ratio, as reported by Mulla et al. [15]. The reaction between NO and H_2 once the trap was regenerated led to a total reduction in NO, as the ($m/e = 30$) signal was maintained below 20 a.u. Consequently, a partial consumption of H_2 was observed, as compared with the ($m/e = 2$) H_2 signal in the absence of NO (Fig. 1b).

Several differences can be observed when the NO_x storage and reduction is carried out at 340 °C (Fig. 2). First, a longer lean period time was needed to saturate the catalyst, which means that higher quantities of NO_x were stored and consequently the formation of larger quantities of products is expected. In fact, the areas under the N_2 and H_2O curves increased by 50% and 62%, respectively. In contrast, the formation of N_2O was negligible and NH_3 formation was only detected after 120 s of regeneration.

The results obtained in the absence of NO during regeneration are in agreement with mechanistic aspects of the regeneration already reported [13–15,18]. The reduction in stored nitrates with hydrogen has been reported to occur by the following reactions:

$$Ba(NO_3)_2 + 8H_2 \rightarrow 2NH_3 + BaO + 5H_2O \quad (1)$$

$$Ba(NO_3)_2 + 5H_2 \rightarrow N_2 + BaO + 5H_2O \quad (2)$$

Lietti et al. [18] reported that during reduction in stored nitrates at 100 °C, reaction (1) accounted for almost all the H_2 consumptions, demonstrating that stored nitrates were reduced efficiently and selectively (>90%) to ammonia. On increasing the reduction temperature, nitrogen formation was promoted due to reaction (3) where the ammonia formed continues to react further with stored nitrates to form nitrogen.

$$3Ba(NO_3)_2 + 10NH_3 \rightarrow 8N_2 + 3BaO + 15H_2O \quad (3)$$

Thus, nitrogen formation involves a two-step pathway: the fast formation of ammonia by reaction of nitrates with H_2 (reaction (1)) and the subsequent reaction of the ammonia formed with stored

[1] For interpretation of colour in Figs. 1–5 and 7–9, the reader is referred to the web version of this article.

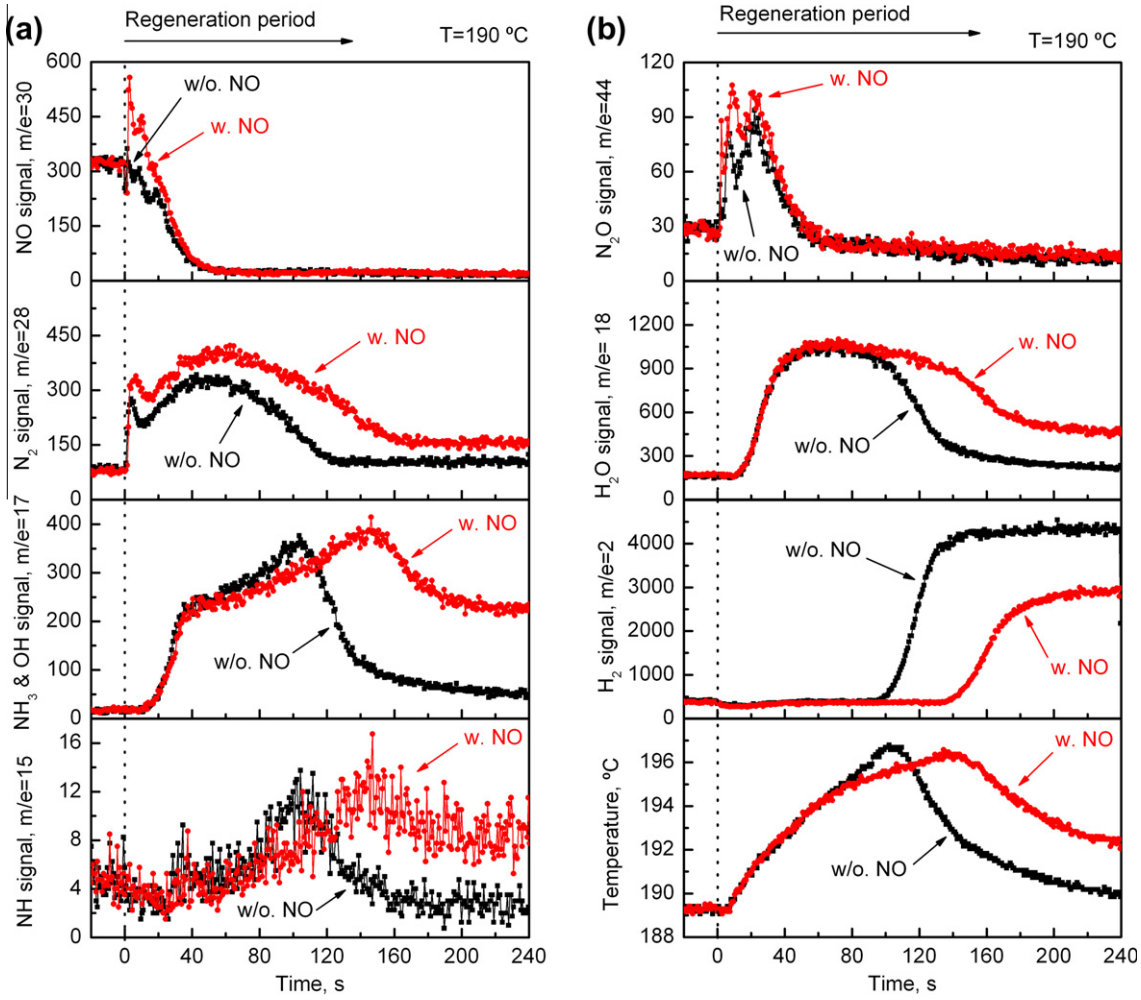

Fig. 1. Evolution of reactants and products during LNT regeneration at 190 °C, in the presence (red points) and in the absence (black points) of NO. (a) NO, N_2, NH_3 and NH; (b) N_2O, H_2O, H_2 and the exit temperature profile. The *Y* axis is shown in arbitrary units, except for the temperature. (For interpretation of the references to colours in this figure legend, the reader is referred to the web version of this paper.)

nitrates leading to the selective formation of N_2 (reaction (3)). This overall mechanism of nitrate reduction during LNT regeneration explains the evolution of products at the reactor exit shown in Figs. 1 and 2 when NO is not fed during regeneration. When the hydrogen front enters the catalyst, the stored NO_x is thought to be converted mainly to ammonia, together with total H_2 consumption. Then, the ammonia formed in the regeneration front reacts further with stored nitrates located downstream to form nitrogen. Thus, the formation of N_2 is detected as soon as the regeneration period starts, but no ammonia can be detected as it is completely consumed. As the regeneration time increases and the hydrogen front moves forward, the ammonia formed has fewer nitrates to react with, and consequently, some NH_3 remains unreacted and is detected at the outlet of the reactor.

The catalyst temperature has been reported to be an important parameter, which determines the extent of ammonia slip [19,26]. When NO_x storage and reduction cycles are carried out at 190 °C (Fig. 1), all the NH_3 formed reacts too slowly with stored nitrates located downstream compared with the residence time in the reactor and, therefore, unreacted NH_3 is observed after 40 s of regeneration. At 340 °C, reaction (3) is much faster and, consequently, NH_3 cannot be detected until 120 s of regeneration, i.e. when N_2 and H_2O signals start to decrease, meaning that the catalyst regeneration is nearly complete and almost no nitrates are present with which NH_3 can react.

When the regeneration of the catalyst is carried out in the presence of NO, as well as reactions (1)–(3), the following reactions may also occur:

$$2NO + 5H_2 \rightarrow 2NH_3 + 2H_2O \quad (4)$$

$$2NO + 2H_2 \rightarrow 2N_2 + 2H_2O \quad (5)$$

The reaction between the incoming NO and H_2 once the trap is regenerated will preferentially lead to the formation of NH_3 due to the presence of excess of hydrogen, with respect to that stoichiometrically needed to reduce all NO. Note that this reaction may also occur during the regeneration in the reactor zones upstream of the hydrogen front, where the catalyst is already regenerated. Consequently, this additional ammonia, apart from that formed from stored nitrates (reaction (1)), may also be involved in the final production of nitrogen via reaction (3).

3.2. LNT regeneration in the presence of (isotopically labelled) ^{15}NO

In an attempt to differentiate the origin of nitrogen production (reaction (3)), that is, via NH_3 formed from stored nitrates (reaction (1)) or via NH_3 formed from reaction between NO and H_2 (reaction (4)), experiments were carried out but feeding ^{15}NO during regeneration instead of ^{14}NO. 15 min was used to saturate the catalyst when the reaction was carried out at 190 °C and 20 min at

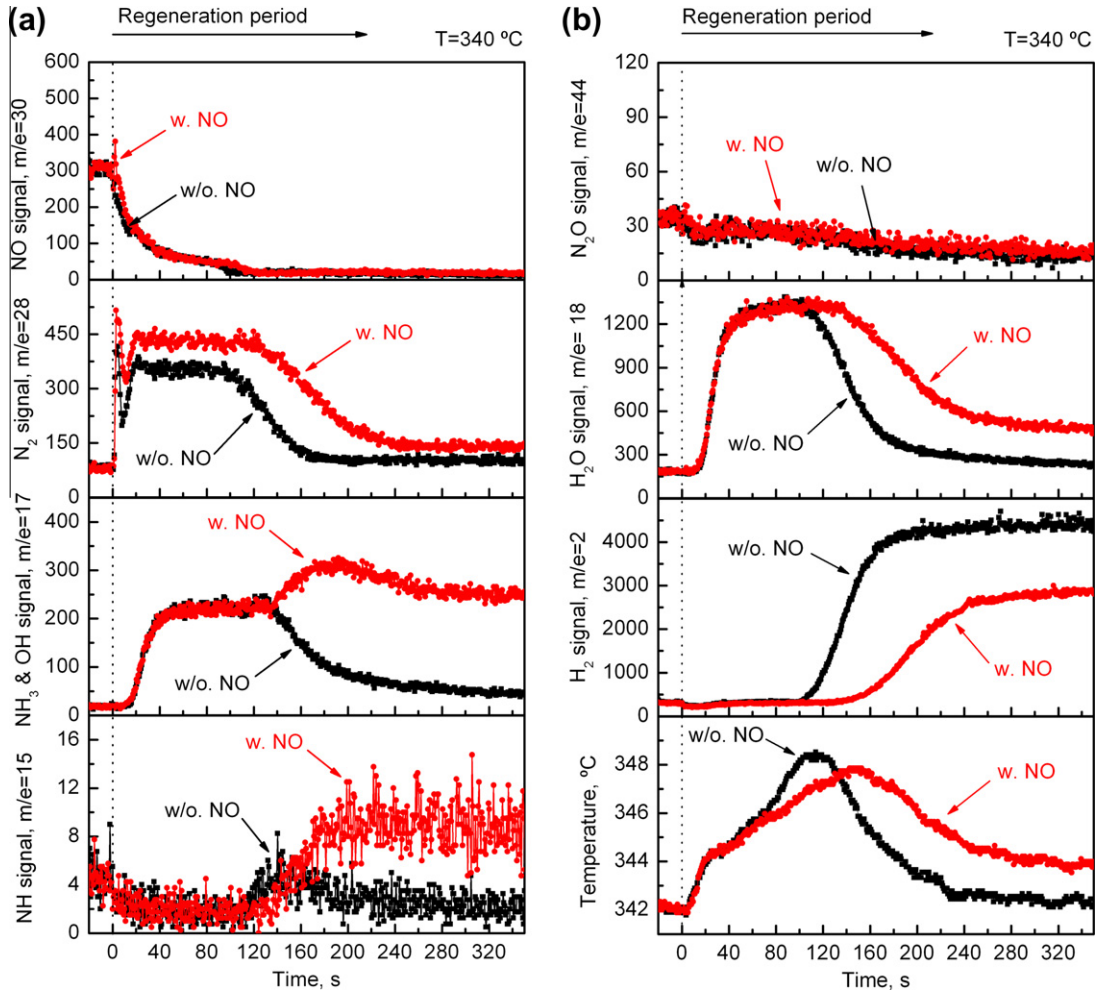

Fig. 2. Evolution of reactants and products during LNT regeneration at 340 °C, in the presence (red points) and in the absence (black points) of NO. (a) NO, N_2, NH_3 and NH; (b) N_2O, H_2O, H_2 and the exit temperature profile. The *Y* axis is shown in arbitrary units, except for the temperature. (For interpretation of the references to colours in this figure legend, the reader is referred to the web version of this paper.)

340 °C. The catalyst was saturated with a gas mixture composed of 800 ppm ^{14}NO, 6% O_2 and Ar to balance. Therefore, all nitrogen stored as nitrates in the catalyst surface will be labelled by ^{14}N. Afterwards, the feedstream was switched to rich conditions containing 800 ppm ^{15}NO, 0.46% H_2 and Ar to balance.

Fig. 3 shows the evolution of $^{15}N_2$ or ^{14}NO ($m/e = 30$), $^{14}N_2$ ($m/e = 28$) and $^{15}N^{14}N$ ($m/e = 29$) signals during LNT regeneration. Fig. 3a shows the evolution of those masses when the reaction was carried out at 190 °C, and Fig. 3b shows the corresponding results at 340 °C. Red points represent the evolution of each component when ^{14}NO is fed during regeneration; black points represent the evolution of the same masses but in the presence of ^{15}NO. In Fig. 3, when unlabelled ^{14}NO is fed during regeneration, the ^{14}NO ($m/e = 30$) reduction pattern as well as the $^{14}N_2$ ($m/e = 28$) formation follows the same behaviour as that shown in Figs. 1 and 2, and the signal corresponding to ($m/e = 29$) remains negligible all over the regeneration period. On the contrary, when ^{15}NO is fed during regeneration, notable differences can be observed. First, the ($m/e = 30$) signal is always higher when ^{15}NO is used instead of ^{14}NO. Second, in the presence of ^{15}NO, the ($m/e = 28$) signal decreases to around a half. Finally, we observe a huge production of the mass ($m/e = 29$).

On the basis of the results shown in Fig. 3, three different pathways for nitrogen formation could be proposed to fit the experimental data. The first route for nitrogen formation involves the reaction between hydrogen and stored nitrates to form $^{14}NH_3$. Note that during the lean period ^{14}NO was fed to the catalyst and, therefore, the stored nitrates are ^{14}N labelled. Thereafter, further reaction of this ammonia with stored nitrates could lead to the final formation of nitrogen ($^{14}N_2$). This is the route already reported in the literature in the absence of NO during regeneration [14,18]. The formation of nitrogen via this route is detected by the ($m/e = 28$) signal.

Route 1:

$$Ba(^{14}NO_3)_2 + 8H_2 \rightarrow 2^{14}NH_3 + BaO + 5H_2O \quad (6)$$

$$3Ba(^{14}NO_3)_2 + 10^{14}NH_3 \rightarrow 8^{14}N^{14}N + 3BaO + 15H_2O \quad (7)$$

The second route for nitrogen formation involves the reaction between the incoming ^{15}NO with H_2 to form $^{15}NH_3$, which again further reacts with stored nitrates (^{14}N labelled) to form nitrogen ($^{14}N^{15}N$ and $^{15}N_2$). This route is detected mainly by the ($m/e = 29$) signal.

Route 2:

$$2^{15}NO + 5H_2 \rightarrow 2^{15}NH_3 + 2H_2O \quad (8)$$

$$3Ba(^{14}NO_3)_2 + 10^{15}NH_3 \rightarrow 6^{14}N^{15}N + 2^{15}N^{15}N + 3BaO + 15H_2O \quad (9)$$

Another third route for nitrogen formation is the direct reaction between incoming ^{15}NO and H_2 to form $^{15}N_2$ (reaction (10)). Note that the reaction between $^{15}NH_3$ formed from reaction (8) which

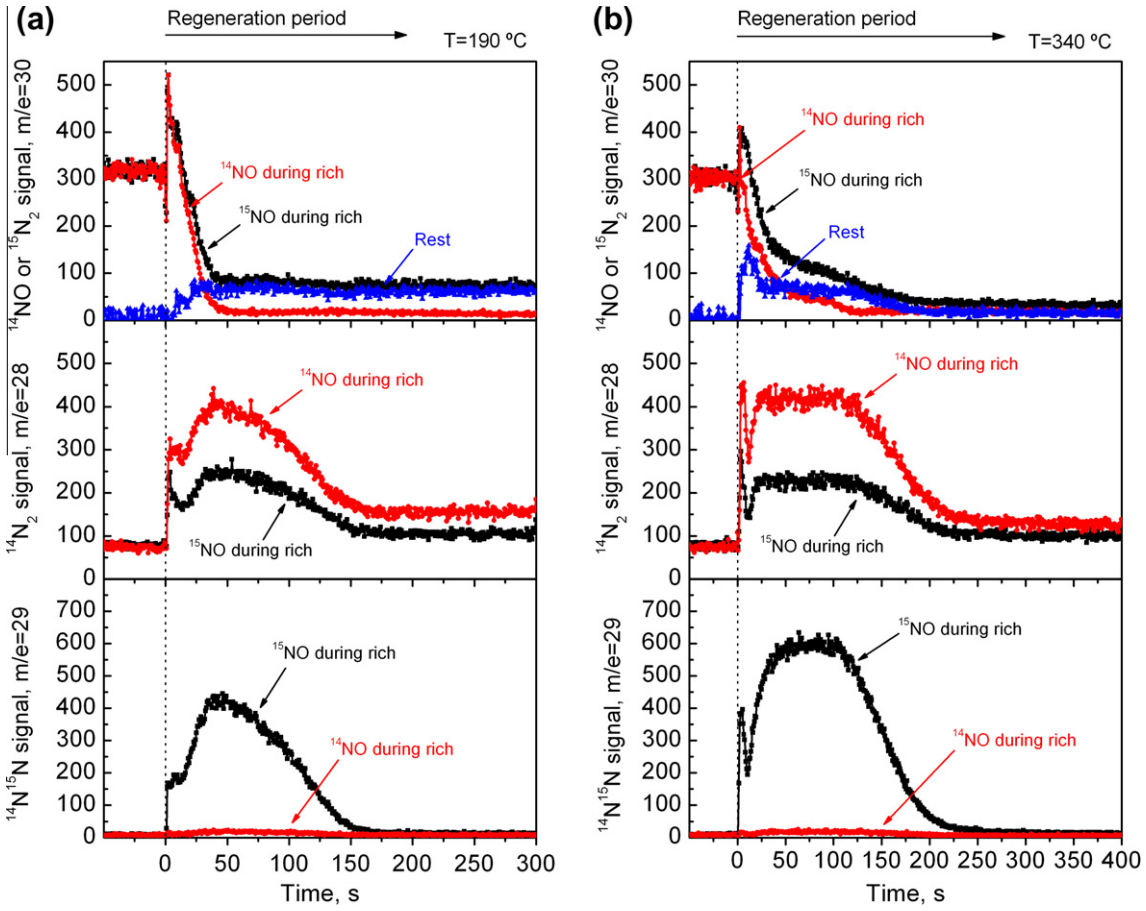

Fig. 3. Evolution of $^{15}N_2$ or ^{14}NO ($m/e = 30$), $^{14}N_2$ ($m/e = 28$) and $^{15}N^{14}N$ ($m/e = 29$) during LNT regeneration, in the presence of ^{14}NO (red points) or ^{15}NO (black points). (a) 190 °C; (b) 340 °C. (For interpretation of the references to colours in this figure legend, the reader is referred to the web version of this paper.)

reacts with ^{15}NO to form $^{15}N_2$ cannot be excluded (reaction (11)). The formation of nitrogen via this route is detected by the ($m/e = 30$) signal.

Route 3:

$$2^{15}NO + 2H_2 \rightarrow {}^{15}N^{15}N + 2H_2O \quad (10)$$

$$4^{15}NH_3 + 6^{15}NO \rightarrow 5^{15}N^{15}N + 6H_2O \quad (11)$$

It is worth noting that when ^{15}NO is fed during the rich period, the mass 30 (black points) would account for the sum of ^{14}NO ($m/e = 30$) being released from the catalyst surface without being reduced and $^{15}N_2$ ($m/e = 30$) being formed due to reactions (9)–(11). However, when the catalyst regeneration is carried out in the presence of ^{14}NO (red points), the ($m/e = 30$) signal only provides the variation in ^{14}NO. The difference between the red and black lines does give the evolution of $^{15}N_2$ and is shown in blue in Fig. 3. As can be observed, at 190 °C, a constant signal around 60 a.u. can be observed after the catalyst has been regenerated due to $^{15}N_2$ formation. On the other hand, at 340 °C, a sharp peak at the initial period of regeneration can be observed (coincident with the "NO_x puff"), decreasing to almost zero for long regeneration times. This means that after the catalyst has been regenerated, the formation of $^{15}N_2$ via reactions (10) and (11) is more favoured at low temperature (190 °C) rather than high temperature (340 °C). However, it has to be kept in mind that $^{15}N_2$ is formed to a much smaller extent in comparison with $^{14}N^{15}N$ and $^{14}N_2$, which are the major nitrogen products.

In summary, the use of ^{15}NO during Pt–Ba/Al_2O_3 catalyst regeneration allowed us to propose three different pathways for nitrogen formation. In fact, all nitrogen detected as $^{14}N_2$ ($m/e = 28$) when ^{14}NO is fed during regeneration can be differentiated as $^{14}N_2$ ($m/e = 28$), $^{14}N^{15}N$ ($m/e = 29$) or $^{15}N_2$ ($m/e = 30$) when ^{15}NO is fed.

3.3. Moving to shorter regeneration periods in the presence of ^{15}NO

In order to move to conditions closer to real operation, shorter NO_x storage and reduction cycles were tested over the Pt–Ba/Al_2O_3 catalyst. As has been already reported, the amount of hydrogen supplied, that is $C_{H2} \times t_{rich}$, determines the extent of NSR catalyst regeneration [15,20]. Consequently, shorter rich period times require higher H_2 concentrations so as to obtain complete regeneration of the catalyst. Therefore, the hydrogen concentration was progressively increased from 0.46% to 3.83% in the presence of 800 ppm of ^{15}NO and Ar to balance. The storage period was 2 min long with a feed composed of 800 ppm ^{14}NO, 6% O_2 and Ar (balance).

Fig. 4 shows the evolution of the ^{14}NO signal during NO_x storage and reduction cycles when the hydrogen concentration fed during the rich period is changed from 0.46% to 3.83%. During the initial period of storage, the ^{14}NO signal value remained practically negligible, meaning that all NO being fed was efficiently stored. Increasing the lean period time, the adsorption sites became progressively saturated and, consequently, the ^{14}NO breakthrough started after 30 s when the reaction was carried out at 190 °C and after 40 s at 340 °C. Once the catalyst had been exposed to the lean gas mixture for 2 min, the feedstream was switched to rich conditions and the ^{14}NO signal decreased gradually to zero. It is worth noting that, as the hydrogen concentration was increased,

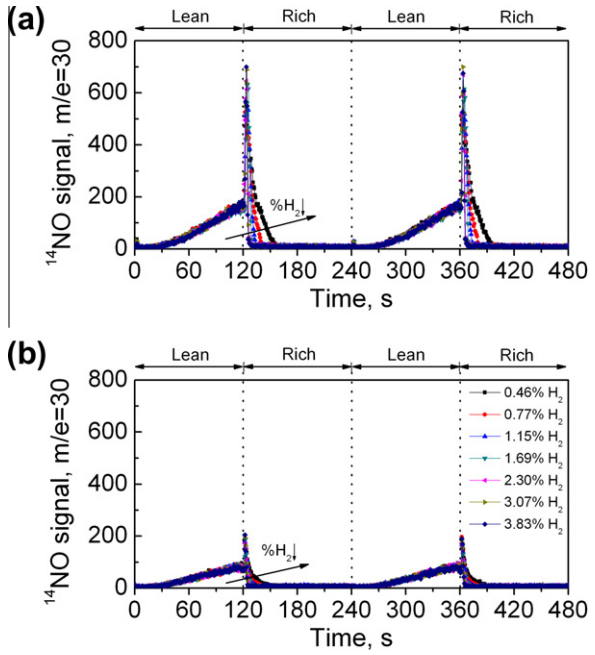

Fig. 4. Evolution of ^{14}NO during two consecutive NO_x storage and reduction cycles for hydrogen concentrations from 0.46% to 3.83% during regeneration. (a) 190 °C; (b) 340 °C. (For interpretation of the references to colours in this figure legend, the reader is referred to the web version of this paper.)

the regeneration of the catalyst occurred faster and, consequently, the ^{14}NO tail became less evident. Considering the cumulative storage behaviour all over the entire lean period, it can be observed that the evolution of ^{14}NO signal is the same for every hydrogen concentration used during regeneration. Therefore, equal amounts of ^{14}NO are expected to be trapped in each experiment.

The evolution of $^{14}N_2$ (m/e = 28), $^{14}N^{15}N$ (m/e = 29) and $^{15}N_2$ (m/e = 30) signals during Pt–Ba/Al_2O_3 catalyst regeneration is shown in Fig. 5. As we have previously reported, the formation of $^{14}N_2$ or $^{14}N^{15}N$ involves the participation of stored nitrates (see reactions (7) and (9)) and, consequently, the evolution of those products follows the extent of catalyst regeneration. Thus, it can be assumed that complete regeneration of the trap is obtained (i.e. no nitrates on the surface) when the formation of $^{14}N_2$ or $^{14}N^{15}N$ decreases to the baseline.

The hydrogen concentration used during the rich period determines the time needed to obtain the complete regeneration of the trap, which is measured by the width of the $^{14}N_2$ or $^{14}N^{15}N$ peak. As the reductant concentration is increased, the regeneration occurs more rapidly, e.g. when the reaction is carried out at 190 °C, 42 s is needed to achieve the complete regeneration of the trap using 0.46% H_2 whereas only 5 s is needed when the hydrogen concentration is increased up to 3.83%. On the other hand, when the reaction is carried out at 340 °C, higher amounts of NO_x are trapped during the lean period (see Fig. 4), and consequently, longer rich period times are needed to regenerate the catalyst, 75 s using 0.46% H_2 and 8 s using 3.83% H_2.

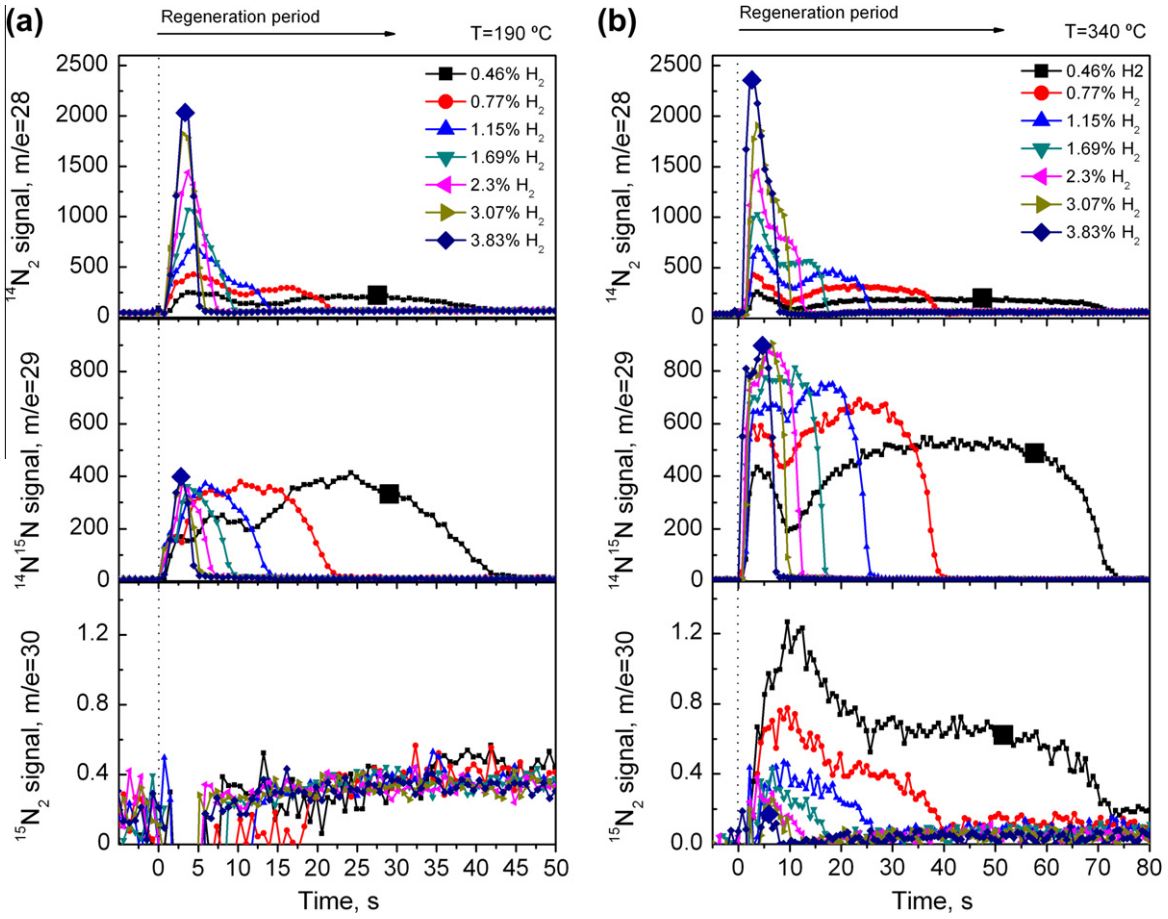

Fig. 5. Evolution of $^{14}N_2$ (m/e = 28), $^{14}N^{15}N$ (m/e = 29) and $^{15}N_2$ (m/e = 30) for hydrogen concentrations from 0.46% to 3.83% during regeneration. (a) 190 °C; (b) 340 °C. (For interpretation of the references to colours in this figure legend, the reader is referred to the web version of this paper.)

Interestingly, the evolution of $^{14}N_2$ and $^{14}N^{15}N$ strongly differs when the hydrogen concentration is increased. On the one hand, for low H_2 concentrations, a broad peak corresponding to $^{14}N_2$ production can be observed. Then, as the hydrogen concentration is increased, the $^{14}N_2$ production peak becomes progressively sharper, decreasing continuously the width of the peak but increasing the maximum value. On the other hand, when the H_2 concentration is increased, the width of the $^{14}N^{15}N$ peak continuously decreases and its maximum value remains constant at 190 °C and slightly increases at 340 °C. In order to observe more clearly the evolution of $^{14}N_2$ and $^{14}N^{15}N$ production when the H_2 concentration is increased, the areas under the curve were calculated in Fig. 5 and plotted in Fig. 6. As it can be observed, the production of $^{14}N_2$ remains fairly constant with increasing hydrogen concentration whereas the production of $^{14}N^{15}N$ is continuously decreasing.

3.4. Discussion

During LNT regeneration, different zones are present in the reactor as explained by Lietti et al. [18]. An initial zone (I), upstream of the H_2 front where the trap is already regenerated; (II) the zone corresponding to the development of the H_2 front, where the reductant concentration decreases to zero due to its fast reaction with stored nitrates; (III) a zone immediately downstream from the H_2 front in which nitrates are present because of the complete H_2 consumption upstream and the last zone (IV) in which the initial nitrate loading is still present. The dynamics of Pt–Ba/Al_2O_3 catalyst during regeneration is greatly influenced by the hydrogen concentration fed, and therefore, the formation and extension of the aforementioned zones is also affected.

Fig. 7 shows the evolution of different zones along the catalyst length with increasing rich period time for low (0.77% H_2) and high (3.03% H_2) reductant concentrations when the regeneration is carried out at 340 °C. As can be observed, the fast transient apparatus used in this study allows us to switch between lean and rich cycles very quickly and, consequently, there is no inert gap between cycles. However, when the transition between oxygen-containing and hydrogen-containing feedstreams reaches the catalyst, hydrogen is totally consumed in the reduction of stored nitrates, leading to an increasing gap between oxygen and hydrogen fronts. Consequently, upstream of the hydrogen front, an oxygen-free zone is formed in which some of the physisorbed or weakly adsorbed NO_x is released due to the decrease in oxygen partial pressure [11,12], contributing to the "NO_x puff" previously described and shown in Fig. 1. As the regeneration time increases, the hydrogen front moves forward leading to the formation of the four zones previously proposed. The extension of each zone was estimated based on Fig. 5. The total regeneration of the catalyst (i.e. when

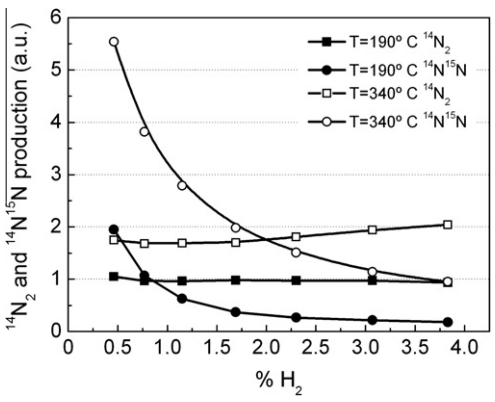

Fig. 6. Production of $^{14}N_2$ and $^{14}N^{15}N$ with H_2 concentration, at 190 °C and 340 °C.

$^{14}N_2$ or $^{14}N^{15}N$ formation decreases to zero) was detected after 40 s for a H_2 concentration of 0.77%. Assuming a homogeneous distribution of nitrates along the catalyst length, the hydrogen front will move forward with a constant velocity. Thus, after 10 s of regeneration, only a quarter of the catalyst will be regenerated. Following the same procedure, the extension of each zone was also calculated for a H_2 concentration of 3.03%.

In zone I, where no nitrates are present on the catalyst surface, platinum will catalyse the reduction in the incoming ^{15}NO with H_2, just as would happen in a steady-state reaction between these two compounds. In order to know the reduction conversion and product selectivity, we performed several steady-state experiments feeding 800 ppm of NO and different hydrogen concentrations from 0.46% to 3.83%, at 190 and 340 °C. In all cases, we observed that NH_3 was the main product of the reaction along with some traces of N_2 whereas the formation of N_2O was negligible. Those results are in agreement with Mulla et al. [15] wherein the selectivity to NH_3 was found to be dependent on the NO/H_2 ratio. The selectivity to NH_3 was favoured with decreasing NO/H_2 ratio, that is, when H_2 is in excess. In fact, when the NO/H_2 ratio was 0.4, the selectivity to NH_3 was 77%. Note that the NO/H_2 ratio used in our experiments was even lower, varying from 0.17 to 0.021, and, therefore, almost 100% selectivity to NH_3 is expected. Thus, the reaction between ^{15}NO and H_2 in zone I will lead to the formation of $^{15}NH_3$ (reaction (8)), which will travel along the catalyst until it reaches the regeneration front. Depending on reaction temperature, NH_3 could be as effective as H_2 in the reduction of stored nitrates. NO_x storage and reduction experiments carried out with mixtures of NH_3 and H_2 during regeneration (not shown) showed that the breakthrough for these two components was coincident in time if the temperature was high enough (340 °C). Consequently, it can be concluded that $^{15}NH_3$ is probably consumed in the regeneration front (zone II) or in the downstream nearby zone (zone III) leading to the formation of $^{14}N^{15}N$ (reaction (9)). On the other hand, at lower temperatures (190 °C), NH_3 breakthrough is detected before H_2, meaning that some NH_3 moves forward through the H_2 front and leaves the catalyst without reacting. Thus, the effectiveness of NH_3 acting as a reductant for stored nitrates decreases with temperature, as previously reported by Lietti et al. [18].

It is obvious that the reaction between ^{15}NO and H_2 to form $^{15}NH_3$ in zone I will gradually progress down the catalyst bed. However, if we assume that the extension of zone I is long enough to obtain total conversion, 800 ppm of $^{15}NH_3$ would be produced and will be continuously reaching the regeneration front. Consequently, one part of the H_2 fed will be consumed in the formation of $^{15}NH_3$, whereas the excess will be used in the reduction of stored nitrates in the regeneration front.

When a low H_2 concentration is used (0.77%), the regeneration front slowly moves forward along the catalyst, i.e. 40 s is needed to obtain the complete regeneration of the catalyst bed (Figs. 5 and 7a). In that case, during all the 40 s of regeneration, the $^{15}NH_3$ formed in zone I will travel along the catalyst bed and will be involved, along with hydrogen, in the reduction of stored nitrates in the regeneration front (zone II) or nearby (zone III). Thus, when low H_2 concentrations are used, the relative importance of $^{15}NH_3$ with respect to H_2 in the reduction of stored nitrates will be noteworthy, and consequently, the formation of $^{14}N^{15}N$ [Route 2, reactions (8) and (9)] will be promoted (see Fig. 6).

On the other hand, when a high H_2 concentration (3.03%) is used, the regeneration front moves forward much faster and, consequently, complete regeneration is obtained in only 10 s (Figs. 5 and 7a). Note that the formation of $^{15}NH_3$ is limited by the concentration of ^{15}NO fed (800 ppm) and consequently the amount of $^{15}NH_3$ acting as reductant would be limited and would be the same irrespective of the H_2 concentration used during the regeneration.

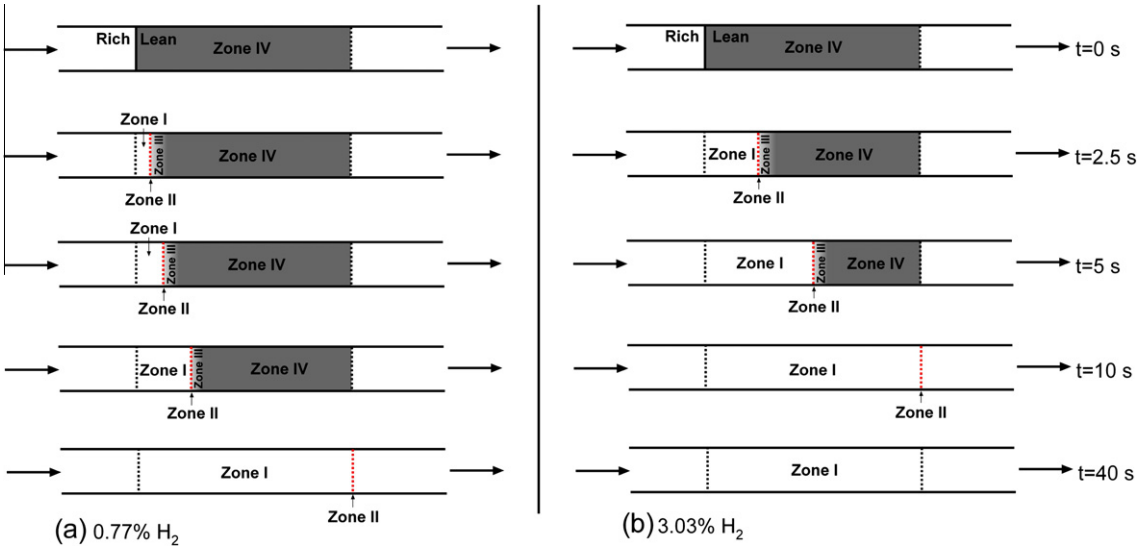

Fig. 7. Evolution of different zones in the LNT with rich period time at 340 °C.

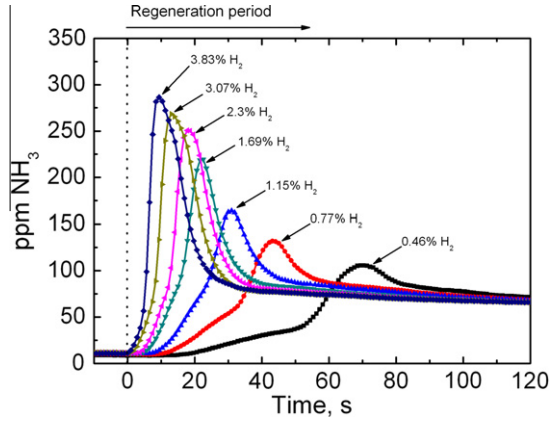

Fig. 8. Evolution of NH_3 during regeneration in the absence of NO, for different H_2 concentrations and 340 °C. (For interpretation of the references to colours in this figure legend, the reader is referred to the web version of this paper.)

Therefore, by increasing the H_2 concentration, the relative importance of $^{15}NH_3$ acting as reductant of stored nitrates with respect to H_2 is reduced, and the production of $^{14}N^{15}N$ decreases as can be observed in Fig. 6. On the other hand, the production of $^{14}N_2$ is almost unaffected by the hydrogen concentration fed during regeneration (Fig. 6). As explained before, when the hydrogen concentration is increased, the relative importance of $^{15}NH_3$ acting as reductant decreases in favour of H_2, and consequently, the formation of $^{14}N_2$ [Route 1, reactions (6) and (7)] should increase. However, our experiments showed that the production of $^{14}N_2$ remains fairly constant with increasing hydrogen concentration. This could be explained by the opposite effect of the reduction selectivity of stored nitrates, favouring the formation of $^{14}NH_3$ at the expense of $^{14}N_2$.

In order to find evidence to support our previous suggestion, we monitored accurately the formation of ammonia during LNT regeneration using an online FT/IR analyser. Fig. 8 shows the evolution of NH_3 when the regeneration was carried out with different H_2 concentrations in the absence of NO at 340 °C. As previously mentioned, increasing the H_2 concentration means that the regeneration of the trap occurred faster and consequently NH_3 was detected earlier in the regeneration period. Furthermore, increasing NH_3 slip was clearly observed, which indicated that

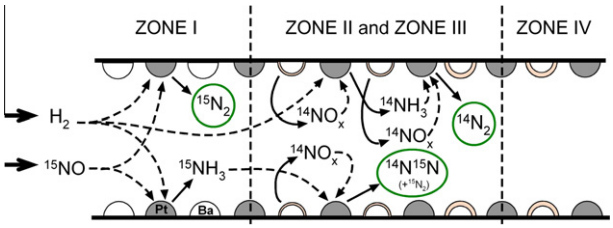

Fig. 9. Schematic of the proposed regeneration mechanism of the LNT with hydrogen. Storage was achieved with ^{14}NO and regeneration in the presence of ^{15}NO.

the formation of NH_3 from stored nitrates is favoured at the expense of nitrogen when the H_2 concentration was increased.

Thus, it can be concluded that two contradictory effects are controlling the formation of $^{14}N_2$, which, in fact, make its rate of production fairly constant. On the one hand, as the H_2 concentration increases, the formation of $^{14}N_2$ is promoted via Route 1. On the other hand, the selectivity of the reduction in stored nitrates towards nitrogen decreases in favour of ammonia.

Fig. 9 shows a schematic of the proposed regeneration mechanism of the trap with hydrogen. The figure illustrates the propagation of the hydrogen front and the interactions with stored $^{14}NO_x$ and incoming ^{15}NO. In the reactor zone where the trap has been regenerated (zone I), the incoming ^{15}NO reacts with H_2 to form $^{15}NH_3$ or $^{15}N_2$ (Route 3). The $^{15}NH_3$ formed will travel along the catalyst until it reaches the regeneration front where it will further react with released $^{14}NO_x$ to form $^{14}N^{15}N$ and $^{15}N_2$ (Route 2). Alternatively, the hydrogen that has not been consumed in the production of $^{15}NH_3$ reacts with released $^{14}NO_x$ to form $^{14}NH_3$. This ammonia can further react with $^{14}NO_x$ on Pt to form $^{14}N_2$ (Route 1). The selectivity of the individual species will depend on the local NO_x/H_2 concentration ratio.

4. Conclusions

The LNT regeneration mechanism proposed in the literature *in the absence of co-fed NO during regeneration*, which involves NH_3 as an intermediate for the final production of nitrogen, has been confirmed. This has now been extended with additional routes for nitrogen formation *when NO is present during the regeneration*, as occurs in a real lean-burn automobile application.

In order to elucidate the role of the incoming NO during the regeneration of LNT and its participation in nitrogen formation, isotopically labelled techniques were employed. During the lean period, the ^{14}NO-containing feedstream was fed to the catalyst, and consequently, all stored nitrates were ^{14}N labelled. During the subsequent rich period, isotopically labelled ^{15}NO was fed. When NO_x storage and reduction cycles were carried out feeding ^{14}NO during both the lean and rich periods, all nitrogen produced in the regeneration period was detected as $^{14}N_2$ ($m/e = 28$). On the other hand, when ^{15}NO was admitted during the regeneration period, three different masses were detected for nitrogen formation, i.e. $^{14}N_2$ ($m/e = 28$), $^{14}N^{15}N$ ($m/e = 29$) and $^{15}N_2$ ($m/e = 30$). On the basis of these results, three different routes for nitrogen formation were deduced: In Route 1, the incoming hydrogen reacts with stored nitrates (^{14}N labelled) to form $^{14}NH_3$, which further reacts with stored nitrates (^{14}N labelled) located downstream to form $^{14}N_2$. In Route 2, the incoming ^{15}NO reacts with hydrogen to form $^{15}NH_3$ upstream of the hydrogen front, that is, in the reactor zone where the trap has been already regenerated. Then, the $^{15}NH_3$ formed travels through the catalyst bed until it reaches the regeneration front where it gets involved in the reduction of stored nitrates (^{14}N labelled) leading to the formation of $^{14}N^{15}N$ ($m/e = 29$). In Route 3, incoming ^{15}NO reacts with hydrogen to form $^{15}N_2$ ($m/e = 30$).

The extension of the different routes for nitrogen formation proposed is affected by the hydrogen concentration and ^{15}NO concentration fed during the regeneration step. First, it is worth noting that the inlet concentration of ^{15}NO is maintained constant for all experiments, leading to a constant formation rate of $^{15}NH_3$ irrespective of the H_2 concentration used. On the other hand, when a low H_2 concentration is used, the regeneration of the trap occurs slowly and, therefore, the total amount of $^{15}NH_3$ acting as reductant will be significant, promoting the formation of $^{14}N^{15}N$. Increasing H_2 concentration results in the decrease in the regeneration time. Consequently, the total amount of $^{15}NH_3$ acting as reductant decreases, i.e. the relative importance of $^{15}NH_3$ acting as reductant of stored nitrates decreases in favour of H_2, what also decreases the formation of $^{14}N^{15}N$. Although this would imply an increase in the production of $^{14}N_2$ via Route 1, in fact this production was experimentally observed to be constant. The explanation offered is that the selectivity of the reduction in stored nitrates towards nitrogen is also affected by hydrogen concentration just in the opposite way, that is, nitrogen selectivity decreases in favour of ammonia with increasing hydrogen concentration. The combination of these two opposed effects makes the production of $^{14}N_2$ fairly constant and independent of the H_2 concentration.

All experiments in this study have been done without feeding water, which however is present in real vehicle application. The potential impact of feeding H_2O to the LNT is under current research in our laboratories.

Acknowledgements

The authors wish to acknowledge the financial support provided by the Spanish Science and Innovation Ministry (CTQ2009-125117) and the Basque Government (Consolidated Research Group, GIC 07/67-JT-450-07). We also gratefully acknowledge the EPSRC for funding this work within the CASTech (EP/G012156) project. One of the authors (BPA) wants to acknowledge to the Spanish Science and Innovation Ministry for the PhD Research Grant.

References

[1] N. Takahashi, H. Shinjoh, T. Iijima, T. Suzuki, K. Yamazaki, K. Yokota, H. Suzuki, N. Miyoshi, S. Matsumoto, T. Tanizawa, T. Tanaka, S. Tateishi, K. Kasahara, Catal. Today 27 (1996) 63.
[2] H. Mahzoul, J.F. Brilhac, P. Gilot, Appl. Catal. B: Environ. 20 (1999) 47.
[3] H.Y. Huang, R.Q. Long, R.T. Yang, Energy Fuels 15 (2001) 205.
[4] S. Salasc, M. Skoglundh, E. Fridell, Appl. Catal. B: Environ. 36 (2002) 145.
[5] S. Erkfeldt, E. Jobson, M. Larsson, Topics Catal. 16 (2001) 127.
[6] T. Kobayashi, T. Yamada, K. Kayano, SAE Tech. Pap. Ser. 97-07-45, 1997.
[7] I. Nova, L. Castoldi, L. Lietti, E. Tronconi, P. Forzatti, F. Prinetto, G. Ghiotti, J. Catal. 222 (2004) 377.
[8] L. Castoldi, I. Nova, L. Lietti, P. Forzatti, Catal. Today 96 (2004) 43.
[9] L. Cumaranatunge, S.S. Mulla, A. Yezerets, N.W. Currier, W.N. Delgass, F.H. Ribeiro, J. Catal. 246 (2007) 29.
[10] V. Medhekar, V. Balakotaiah, M.P. Harold, Catal. Today 121 (2007) 226.
[11] W.S. Epling, L.E. Campbell, A. Yezerets, N.W. Currier, J.E. Parks, Catal. Rev. Sci. Eng. 46 (2004) 163.
[12] Z.Q. Liu, J.A. Anderson, J. Catal. 224 (2004) 18.
[13] I. Nova, L. Lietti, L. Castoldi, E. Tronconi, P. Forzatti, J. Catal. 239 (2006) 244.
[14] I. Nova, L. Lietti, P. Forzatti, Catal. Today 136 (2008) 128.
[15] S.S. Mulla, S.S. Chaugule, A. Yezerets, N.W. Currier, W.N. Delgass, F.H. Ribeiro, Catal. Today 136 (2008) 136.
[16] P. Forzatti, L. Lietti, I. Nova, E. Tronconi, Catal. Today 151 (2010) 202.
[17] J. Pihl, J. Parks, S. Daw, T. Root, SAE Tech. Pap. Ser. 2006-01-3441, 2006.
[18] L. Lietti, I. Nova, P. Forzatti, J. Catal. 257 (2008) 270.
[19] B. Pereda-Ayo, D. Duraiswami, J.A. González-Marcos, J.R. González-Velasco, Chem. Eng. J. 169 (2011) 58.
[20] B. Pereda-Ayo, D. Duraiswami, J.J. Delgado, R. López-Fonseca, J.J. Calvino, S. Bernal, J.R. González-Velasco, Appl. Catal. B: Environ. 96 (2010) 329.
[21] J.P. Breen, R. Burch, C. Fontaine-Gautrelet, C. Hardacre, C. Rioche, Appl. Catal. B: Environ. 81 (2008) 150.
[22] A. Kumar, M.P. Harold, V. Balakotaiah, J. Catal. 270 (2010) 214.
[23] B. Pereda-Ayo, R. López-Fonseca, J.R. González-Velasco, Appl. Catal. A: Gen. 363 (2009) 73.
[24] J.P. Breen, C. Rioche, R. Burch, C. Hardacre, F.C. Meunier, Appl. Catal. B: Environ. 72 (2007) 178.
[25] W.P. Partridge, J.S. Choi, Appl. Catal. B: Environ. 91 (2009) 144.
[26] I. Nova, L. Castoldi, L. Lietti, E. Tronconi, P. Forzatti, Topics Catal. 42–43 (2007) 21.